GOSPODARKA SUROWCAMI MINERALNYMI – MINERAL RESOURCES MANAGEMENT

2026 Volume 42 Issue 2 Pages 89–111

DOI: 10.24425/gsm.2026.1426

MONIKA CHUCHRO[1], BARBARA BIELOWICZ[2]

Descriptive and predictive analysis of trace metals in coal ash: statistical insights and modeling

Introduction

Coal ash, particularly fly ash and bottom ash, is a significant environmental concern due to its heavy metal content. It can also serve as a secondary source of critical raw materials, such as gallium, cobalt, and vanadium. Understanding the behavior of these trace elements in ash is essential for environmental safety, recycling, and the development of circular economy strategies. The distribution of elements in ash depends on combustion conditions, coal type, and mineralogical composition.

Trace metals in coal and its combustion residues encompass both valuable and potentially toxic elements (PTEs), such as copper (Cu), cobalt (Co), nickel (Ni), vanadium (V), antimony (Sb), molybdenum (Mo), zinc (Zn), silver (Ag), and gallium (Ga). The selection of these nine elements was based on their dual significance: several of them (Co, Ga, V, Sb) are classified by the European Commission as Critical Raw Materials due to their strategic importance and

✉ Corresponding Author: Monika Chuchro; e-mail: chuchro@agh.edu.pl
[1] AGH University of Krakow, Poland; ORCID iD: 0000-0002-0381-4697; e-mail: chuchro@agh.edu.pl
[2] AGH University of Krakow, Poland; ORCID iD: 0000-0002-8742-5890; e-mail: bbiel@agh.edu.pl

supply risk, while the remaining elements (Cu, Ni, Zn, Mo, Ag) represent potentially toxic or technologically valuable metals commonly associated with coal combustion residues. Elements such as As, Pb, and Hg, although environmentally relevant, were intentionally excluded because they have been extensively studied in previous works, whereas this study focuses on less commonly modeled trace and critical elements. Others, such as As, Pb, and Hg, are known environmental pollutants that can infiltrate ecosystems and affect human health (Dai and Finkelman 2018).

Understanding the concentration and distribution of these metals in various coal deposits and corresponding ashes is crucial for environmental management and resource recovery. Fly ash, a fine particulate matter, is known to be enriched in specific trace elements, often at levels exceeding their concentrations in the original coal (Pan et al. 2018). As global concerns about environmental pollution and sustainable resource utilization grow, the recovery of valuable trace metals from coal combustion products presents an opportunity for transitioning towards a circular economy (Dagwar et al. 2025).

The concept of extracting critical elements from coal ashes was initially explored in the context of Russian coal ashes (Seredin 1996). The investigation of critical raw materials in coal and its corresponding ashes has been predominantly undertaken by Chinese researchers, who have focused on the presence of critical elements in coal deposits (Dai and Finkelman 2018). A comprehensive analysis of critical raw materials in coal has been conducted by various research groups, including, for example, Dai et al. (2012) and Lefticariu et al. (2020). Furthermore, the content of critical raw materials in coal ashes has been extensively examined by numerous researchers, such as Dai et al. (2012), Franus et al. (2015), and Bielowicz et al. (2018). A thorough review of the existing literature on the concentration of critical elements in coal and its ashes unequivocally indicates that additional research is necessary to further elucidate this topic. The current state of knowledge highlights the need for continued investigation into the occurrence, distribution, and recovery of critical raw materials from coal combustion residues, which is essential for ensuring a sustainable supply of these vital elements.

The combustion process concentrates non-volatile metals in the resulting ashes. For example, at an ash content level of 12.5%, non-volatile metals are expected to occur at eight times higher levels in Coal Combustion Residuals (CCRs) compared to the source coal. Fly ash, a primary component of CCRs, is typically enriched in elements such as arsenic, boron, and lead, whereas flue gas desulfurization (FGD) residues and boiler slag are more enriched in mercury (Izquierdo et al. 2013).

Investigations of coal fly ash from Poland have revealed higher concentrations of cadmium (Cd), lead (Pb), zinc (Zn), and barium (Ba) compared to the original coal. Enrichment factors for these elements in the ash have been determined, indicating that elements such as Ba, nickel (Ni), and uranium (U) are volatile and can condense on ash particles in varying amounts. This enrichment poses potential environmental risks, particularly when ashes are utilized as soil amendments or construction materials (Zhang et al. 2018). The mobilization of these trace metals during combustion and their subsequent concentration in CCRs

highlights the need for careful management and utilization of coal ashes to mitigate potential environmental hazards.

The presence of trace metals in coal and coal ash has significant environmental and health implications. For instance, in Mooresville, North Carolina, concerns have been raised regarding the link between buried coal ash and increased incidence of thyroid cancer. Coal ash contains hazardous substances such as arsenic and heavy metals that can leach into the environment, posing a threat to human health (Harkness et al. 2015). On the other hand, critical metals like gallium (Ga), cobalt (Co), and molybdenum (Mo) are essential for the production of modern electronics, wind turbines, and lithium-ion batteries. Their recovery from coal ash can reduce dependence on primary sources and contribute to resource security. Research has demonstrated that hydrometallurgical and biotechnological methods can effectively recover metals from ash through acid leaching or metal-oxidizing bacteria (Quina et al. 2018).

Existing recovery technologies also include physicochemical methods such as electrostatic separation, flotation, and hydrometallurgical and pyrometallurgical processes. For example, vanadium (V) can be recovered from coal ash through alkaline leaching, enabling its utilization in the steel and chemical industries (Font et al. 2007). Despite the significant potential for metal recovery from coal ash, technological and economic challenges persist. High extraction process costs and variable metal content in ash limit their commercial viability. On the other hand, the development of innovative methods such as biotechnology, nanofiltration, and selective ion extraction can enhance metal recovery efficiency and contribute to the growth of a circular economy (Joshi et al. 2025).

Conversely, inadequate coal waste management can lead to water and soil pollution, impacting ecosystems and human health. Therefore, understanding the distribution of trace metals in coal and coal ash is crucial for developing effective strategies for their safe utilization and resource recovery. The application of circular economy (CE) concepts in managing coal ash and trace metals is becoming increasingly important in the context of global sustainability challenges. The primary objective of CE is to minimize waste through reuse, recycling, and resource recovery (Gaustad et al. 2021).

In this regard, the recovery of critical metals from coal ash can be seen as a key component of a circular economy approach, enabling the reduction of primary raw material extraction and promoting sustainable development. Furthermore, the integration of biotechnology and nanotechnology can enhance the efficiency of metal recovery processes, making them more economically viable and environmentally friendly (Quina et al. 2018). As the world transitions towards a more sustainable and resource-efficient future, the importance of recovering valuable metals from coal ash will continue to grow, driving innovation and investment in this field. Ultimately, a comprehensive understanding of trace metal distribution in coal and coal ash is essential for developing effective strategies for their safe utilization, recovery, and management, minimizing environmental impacts while promoting resource security and sustainability.

This paper aims to characterize the trace metal content in ash, examine its geochemical relationships, and apply statistical modeling to predict metal concentrations from oxide

content. The novelty of this study lies in the application of both classical regression and machine-learning-based SVM models to multi-rank Polish coal ash datasets, which has not been previously reported at this scale. In contrast to earlier Polish studies focusing mainly on concentration levels and environmental aspects, this work integrates predictive modeling with geochemical interpretation, providing a new methodological framework for assessing trace metal behavior and recovery potential from coal ashes. The nine trace elements selected for this study (Sb, Cu, Co, Ga, Ni, V, Mo, Ag, Zn) are investigated due to their dual relevance: several are classified by the European Commission as Critical Raw Materials (Co, V, Sb, Ga), and the remaining represent environmentally regulated or technologically valuable metals frequently considered for extraction from coal-derived waste streams. Previous Polish studies have generally focused on concentration ranges and environmental behavior of metals in ash; however, machine-learning-based prediction models have not yet been applied to multi-rank coal ash datasets at this scale. This work therefore, introduces a combined geochemical-statistical analysis designed to quantify metal behavior, identify oxide-metal relationships, and evaluate predictive performance.

1. Materials and methods

1.1. Materials and data

Ash samples were generated from 28 coal samples, representing lignite (L), subbituminous (SB), and bituminous (B) ranks from various Polish coal basins (Table 1). These ashes were

Table 1. Origin of coal samples

Tabela 1. Pochodzenie próbek węgla

Rank	Sample No	Deposit
Lignite	1L – 3L	Pątnów V
	4L – 5L	Turów
	6L – 7L	Sieniawa
	8L – 10L	Bełchatów
	11L – 12L	Szczerców
Subbituminous coal	1SB	Poręba
Bituminous coal	1B	Jas-Mos
	2B – 5B	Janina
	6B – 11B	Bogdanka
	12B – 13B	Wesoła
	14B – 15B	Bielszowice

analyzed for nine trace metals: antimony (Sb), copper (Cu), cobalt (Co), gallium (Ga), nickel (Ni), vanadium (V), molybdenum (Mo), silver (Ag), and zinc (Zn). All samples were full-depth cut samples, in accordance with the PN-G-04502:2014-11 standard.

1.2. Analytical approach

To elucidate the fundamental properties of the collected samples, both proximate and ultimate analyses were performed, providing insight into their physical and chemical characteristics. Furthermore, the chemical composition of the ash was examined, as well as the elemental distribution in both coal and ash, by the accredited Bureau Veritas Minerals Laboratory, Vancouver. To facilitate precise determination of trace elements, inductively coupled plasma mass spectrometry (ICP-MS) analysis was conducted on samples digested with a modified aqua regia solution (1:1:1 HNO_3/HCl/H_2O), enabling the detection of elements at low to ultra-low concentrations in both coal and ash. This analytical approach allowed for the sensitive and accurate quantification of trace elements, including those present at concentrations below 1 μg/g.

The dataset for the ash samples is partially incomplete. Complete data are available for cobalt (Co), gallium (Ga), and vanadium (V). However, for each of the remaining six elements, seven data gaps (I.S.) were identified, representing 25% of the observations for each element.

1.3. Statistical analysis

A comprehensive statistical analysis was performed to assess inter-element relationships in coal and ash samples. This included the computation of descriptive statistics and the generation of correlation matrices for both material types (Marshall and Jonker 2010). To characterize the relationships between variables, Pearson's correlation coefficient (R) and Spearman's rank correlation coefficient (S) were calculated. These measures facilitated the assessment of the presence, direction, strength, and form of associations, offering insights into underlying geochemical patterns (Hauke and Kossowski 2011). Additionally, correlations between oxide contents in ash and elemental concentrations in coal ash were examined to identify potential compositional linkages.

Beyond exploratory analyses, multiple linear regression models with hyperparameter optimization and support vector machine (SVM) models were constructed to characterize the complex interactions between trace elements in ash. The preliminary selection of independent variables was informed by statistically significant relationships identified in Spearman's rank correlation matrix, while the final variable selection and model specification were performed using automated procedures of independent variables testing combined with hyperparameter tuning to optimize model performance. These models were designed to determine the most significant predictors of metal concentrations in ash based on their

levels in coal (Akinyemi et al. 2020). Model performance was evaluated using standard metrics: coefficient of determination (R^2), mean absolute percentage error (MAPE), and root mean square error (RMSE).

All computations were carried out in the R programming environment (version 4.4.2) using RStudio (version 2024.09.1 Build 394). A suite of specialized packages was employed for data processing, visualization, and modeling, including: dplyr (v1.1.4), e1071 (v1.7-16), ggplot2 (v3.5.1), leaps (v3.2), and MLmetrics (v1.1.3), providing a robust analytical framework for descriptive statistics, correlation assessment, and regression modeling.

2. Results

2.1. Descriptive statistics

Elemental concentrations in ash samples reveal notable compositional shifts relative to their parent coal (Figure 1, Appendix 1). Specifically, cobalt, gallium, vanadium, and copper exhibit proportional increases compared with parent coal.

The total concentration of analyzed elements for samples with all identified elements ranges from 284.2 ppm for sample 1L to 2576.3 ppm for sample 15B. The average concentration of analyzed elements in the samples (excluding those with missing data) is 867.7 ppm for lignite and 1227.7 ppm for bituminous coal (Figure 1). The distinctly higher total trace metal content observed in bituminous coal ashes may be linked to the greater contribution of sulfide

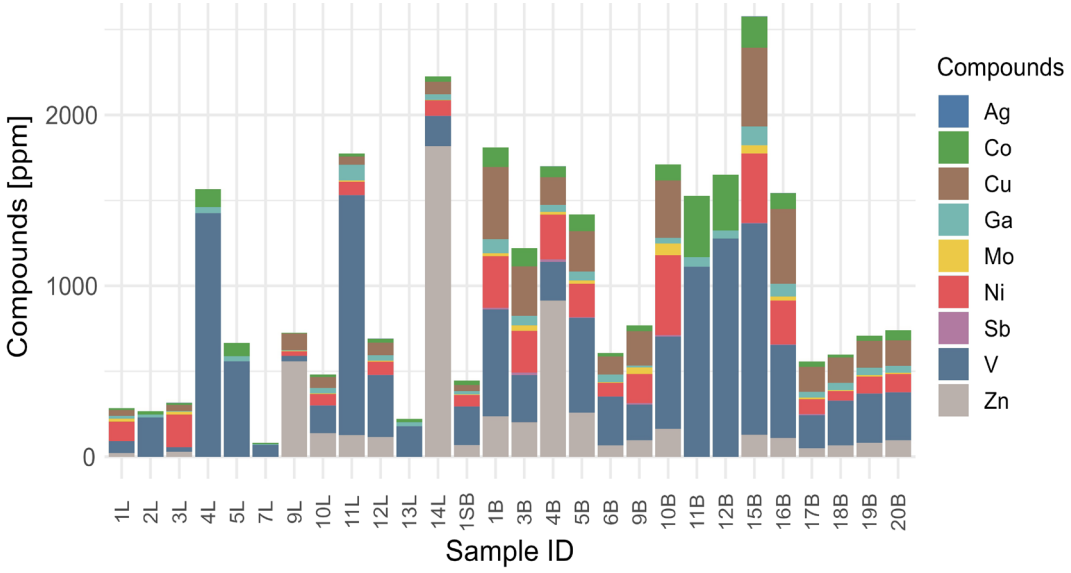

Fig. 1. Metals concentration in individual samples

Rys. 1. Zawartość metali w poszczególnych próbkach

mineral phases and a higher degree of coalification, which promotes stronger metal binding in the organic matrix prior to combustion. In contrast, lower total contents in lignite-derived ashes likely reflect dilution by carbonate and clay minerals, as well as lower original metal concentrations in low-rank coals. Outlier profiles persist in samples 14L, 7L, and 13L, which continue to deviate significantly from the remaining dataset.

Excluding zinc, the average concentrations of trace elements in ash are higher for samples derived from bituminous coal. This pattern suggests that the enrichment of most trace metals is enhanced by increasing coal rank, which is consistent with the progressive concentration of organically bound and sulfide-associated elements during coalification. The reverse trend observed for zinc indicates a different geochemical control, likely related to its stronger association with detrital mineral phases and carbonate components that are more abundant in lignite. These findings indicate a substantial redistribution of elements during combustion, resulting in altered geochemical signatures in the ash. The observed variation may stem from differences in geological provenance, mineralogical composition, or combustion parameters. Further investigation into these factors is warranted to clarify the mechanisms influencing elemental behavior in ash and to evaluate the potential for industrial utilization or environmental remediation of specific ash types.

Ash samples exhibited high variability in trace metal concentrations. Such large dispersion likely reflects differences in mineralogical composition of the parent coals, variable contribution of sulfide and aluminosilicate phases, as well as differing combustion conditions, which jointly control metal volatilization, condensation, and final distribution in ash. The extreme zinc enrichment observed in selected samples may indicate localized sphalerite mineralization or secondary condensation from the flue gas phase. For instance, Zn ranged from 22 to 1818 ppm, Co varied from 4.3 to 360 ppm, and V reached a maximum of 1426 ppm with a minimum of 27 ppm.

High variability in zinc concentrations, including an extreme outlier in sample 14L, indicates potential nonlinear behavior or the presence of geochemically distinct ash types, suggesting the need for adaptive modeling approaches. Such extreme zinc enrichment may reflect the presence of localized Zn-rich mineralization (e.g., sphalerite) in the parent coal seams or intensive secondary condensation of volatilized zinc from the flue gas onto fine ash particles during cooling. Elevated cobalt and vanadium variability may additionally indicate variable contributions of mafic detrital material and clay minerals, which are known to preferentially host these elements. These processes jointly explain the strong non-linearity observed in statistical relationships and justify the application of machine-learning-based modeling techniques. Elevated coefficients of variation for elements such as Co, Mo, and Zn support the hypothesis of heterogeneity in coal origins or combustion conditions.

The primary parameters characterizing the examined ash samples, encompassing descriptive statistical analysis outcomes as well as elemental composition distributions, are compiled in Table 2. These datasets furnish an exhaustive representation of the attributes inherent to the scrutinized coal samples, thereby establishing a basis for subsequent in-depth examination and elucidation of the findings.

Table 2. Results of descriptive statistics for coal ash (ppm)

Tabela 2. Wyniki statystyk opisowych dla popiołów węgla (ppm)

Compound	All samples				Lignite samples				Bituminous coal samples				Clarke
	Min	Mean	Median	Sd	Min	Mean	Median	Sd	Min	Mean	Median	Sd	
	Max				Max				Max				
Sb	0.2	4.1	1.6	4.7	0.2	0.6	0.6	0.3	1.3	6.2	5.0	4.9	1.2
	14.9				1.2				14.9				
Co	4.3	71.0	30.8	88.3	4.3	28.3	18.0	30.6	15.8	108.2	92.7	105.4	25.0
	360.0				104.7				360.0				
Cu	34.2	177.0	148.8	136.2	34.2	60.6	63.2	22.7	106.8	250.4	201.5	125.3	60.0
	461.0				96.9				461.0				
Ga	3.9	39.6	34.1	26.0	3.9	27.2	27.0	24.0	11.5	50.9	44.4	23.6	12.0
	110.4				93.7				110.4				
Mo	2.8	17.2	11.5	16.9	2.8	8.4	6.9	6.1	3.6	23.0	17.3	19.0	1.5
	68.7				17.3				68.7				
Ni	26.5	163.5	106.1	118.5	26.5	91.4	77.5	51.0	54.6	209.7	194.9	129.0	84.0
	466.2				190.6				466.2				
Ag	0.1	0.6	0.3	0.5	0.1	0.1	0.1	0.1	0.3	0.8	0.9	0.5	0.1
	1.9				0.2				1.9				
V	27.0	458.2	278.5	429.1	27.0	391.3	177.0	501.3	193.0	527.1	287.0	380.6	120.0
	1,426.0				1,426.0				1,277.0				
Zn	22.0	254.7	116.0	404.4	22.0	401.1	126.0	650.8	50.0	190.2	110.0	227.5	70.0
	1,818.0				1,818.0				914.0				

Notably, all analyzed elements exhibit high variability in their concentrations, with frequent occurrences of outliers and higher mean values compared to medians. The average concentration of elements in the analyzed samples is higher than the Clarke values for each element. In the case of nickel, the average concentration in the samples is twice as high, while for the remaining elements, it is several times higher (Table 2). When analyzing the coal types separately, coal combustion residuals (CCRs), it can be observed that, for antimony and silver, the average concentration in the samples is lower than or equal to the Clarke values for lignite. For the other elements, the values are significantly higher than the Clarke values for both lignite and bituminous coal ash.

Comparing lignite and bituminous coal ash, it can be noted that lower minimum values for lignite were observed for all analyzed elements. Additionally, the maximum values are generally lower for lignite, with the exception of vanadium and zinc. Similarly, the average values are typically lower for lignite, except for zinc. The medians are lower than the mean values for both coal types, except for silver in bituminous coal, indicating the presence of distribution disturbances, specifically outliers. Furthermore, for cobalt, gallium (L), molybdenum (B), vanadium (L), and zinc, the standard deviation is higher or similar to the mean value, which suggests very high variability within the dataset (Table 2). Such extreme dispersion reflects strong geochemical heterogeneity of the studied coal ashes and confirms that trace metal distribution is controlled by multiple overlapping factors, including coal rank, mineralogical composition, combustion temperature, and physicochemical behavior during volatilization and recondensation. From a practical perspective, this variability directly limits the predictability of average-based models and highlights the necessity of site-specific assessments for both environmental risk evaluation and raw material recovery potential.

2.2. Correlation analysis

The correlation analysis assumed a statistical significance level of 0.05. For 28 pairs of observations (Ga, Co, V), correlations with absolute values greater than or equal to 0.37 were considered statistically significant. For 21 pairs of observations (Ag, Cu, Sb, Mo, Ni, Zn), correlations with absolute values greater than or equal to 0.44 were considered statistically significant. The correlation results are presented in Table 3.

Antimony (Sb) exhibits non-parametric Spearman correlations with other elements, suggesting the presence of non-linear relationships or multiple outlier values in the analyzed sample. Antimony is not correlated with zinc, while its correlations with other elements range from 0.47 (Ga) to 0.88 (Ag).

Cobalt (Co) displays mixed correlation patterns, with some linear relationships and others non-parametric. Linear correlations are observed with copper, gallium, molybdenum, nickel, and silver (highest R: 0.96). In contrast, correlations with antimony and vanadium are non-parametric. Cobalt is not significantly correlated with zinc.

Similar to cobalt, copper (Cu) exhibits mixed correlation patterns. Correlations with cobalt, gallium, molybdenum, nickel, and silver are linear, while those with other elements are non-parametric. The highest correlation for copper is 0.91, which corresponds to a correlation with silver.

Gallium (Ga) displays linear correlations with cobalt, copper, nickel, silver, and vanadium, as well as non-parametric correlations with antimony. Correlations with molybdenum and zinc are not statistically significant. The most significant correlation is found to exist between gallium and vanadium, characterized by a strong positive linear association with a correlation coefficient of 0.88.

Molybdenum (Mo) exhibits the strongest linear correlation (0.88) with nickel. In addition to this correlation, molybdenum is linearly correlated with cobalt, copper, and silver. A non-parametric relationship is observed with antimony, while correlations with gallium, vanadium, and zinc are not statistically significant.

Nickel (Ni) displays similar correlation patterns to molybdenum, with primarily linear relationships. Nickel is non-parametrically correlated with antimony and is not significantly correlated with vanadium or zinc. The strongest correlation for nickel is with molybdenum, exhibiting a linear relationship with a correlation coefficient of 0.88.

Silver (Ag) exhibits distinct correlation patterns, similar to those of cobalt and copper. It is correlated with gallium and vanadium, with the correlation with gallium being linear (difference between correlations <0.02). The correlation with vanadium is non-parametric.

Vanadium (V) displays a strong linear correlation with gallium (0.88), which is the strongest correlation for this element. Other correlations are non-parametric. Vanadium is not correlated with zinc (Zn), which is not significantly correlated with any of the other analyzed elements.

In summary, relationships with antimony and vanadium often exhibit non-parametric characteristics, while correlations with zinc are typically absent. For some elements, correlations with vanadium are also absent. The remaining elements display linear correlations. Silver and nickel exhibit strong and very strong correlations, with four correlations exceeding 0.8, indicating strong relationships with most elements.

The correlations between the analyzed elements and oxides exhibit mixed relationships, similar to those observed for the element-element correlations (Tables 3, 4). The elements do not show statistically significant correlations with SiO_2 and MgO. Statistically significant correlations are both positive and negative.

The strongest correlation observed is the relationship between gallium and Al_2O_3 (0.73). Positive correlations are found between elements and Al_2O_3, Fe_2O_3, Na_2O, K_2O, TiO_2, P_2O_5, and Cr_2O_3. The strongest correlations occur for Al_2O_3 and are linear with cobalt, copper, and non-parametric with gallium, silver, and vanadium (Table 4).

In the case of Fe_2O_3, a linear correlation is observed for antimony, molybdenum, and nickel, and this oxide also has statistically significant non-parametric relationships with cobalt, copper, and zinc. Correlations with CaO are mixed in nature, as the correlation with antimony and nickel is a non-parametric negative correlation, whereas correlations between CaO

Table 3. Correlation matrices

Tabela 3. Macierz korelacji

Compound	Sb		Co		Cu		Ga		Mo		Ni		Ag		V		Zn	
	R	S	R	S	R	S	R	S	R	S	R	S	R	S	R	S	R	S
Sb	–	–	0.54	0.83	0.52	0.84	0.19	0.47	0.55	0.68	0.62	0.70	0.62	0.88	0.07	0.48	0.11	0.34
Co	0.54	0.83	–	–	0.90	0.86	0.70	0.61	0.66	0.64	0.84	0.78	0.96	0.90	0.55	0.63	–0.03	0.43
Cu	0.52	0.84	0.90	0.86	–	–	0.64	0.59	0.67	0.68	0.81	0.71	0.87	0.91	0.46	0.59	–0.11	0.40
Ga	0.19	0.47	0.70	0.61	0.64	0.59	–	–	0.22	0.27	0.44	0.39	0.65	0.67	0.88	0.86	–0.09	0.28
Mo	0.55	0.68	0.66	0.64	0.67	0.68	0.22	0.27	–	–	0.88	0.84	0.68	0.69	0.32	0.38	–0.17	0.09
Ni	0.62	0.70	0.84	0.78	0.81	0.71	0.44	0.39	0.88	0.84	–	–	0.84	0.74	0.41	0.41	–0.04	0.25
Ag	0.62	0.88	0.96	0.90	0.87	0.91	0.65	0.67	0.68	0.69	0.84	0.74	–	–	0.52	0.65	–0.02	0.34
V	0.07	0.48	0.55	0.63	0.46	0.59	0.88	0.86	0.32	0.38	0.41	0.41	0.52	0.65	–	–	–0.16	0.24
Zn	0.11	0.34	–0.03	0.43	–0.11	0.40	–0.09	0.28	–0.17	0.09	–0.04	0.25	–0.02	0.34	–0.16	0.24	–	–

R – Pearson's linear coefficient, S – Spearman's rank correlation coefficient.

Table 4. Correlations matrix with oxides

Tabela 4. Macierz korelacji z tlenkami

Compound	SiO_2		Al_2O_3		Fe_2O_3		MgO		CaO		Na_2O		K_2O		TiO_2		P_2O_5		MnO		Cr_2O_3	
	R	S	R	S	R	S	R	S	R	S	R	S	R	S	R	S	R	S	R	S	R	S
Sb	–0.29	–0.18	0.18	0.44	0.61	0.54	0.17	0.25	–0.37	–0.47	0.63	0.68	0.00	0.40	–0.27	–0.09	–0.02	0.56	0.17	–0.18	0.04	0.35
Co	–0.01	–0.03	0.59	0.54	0.27	0.50	–0.22	–0.08	–0.48	–0.49	0.33	0.50	0.05	0.33	0.08	0.12	0.37	0.54	–0.27	–0.45	0.04	0.34
Cu	–0.07	–0.05	0.66	0.65	0.34	0.46	–0.21	–0.05	–0.52	–0.52	0.18	0.57	0.05	0.37	0.07	0.10	0.43	0.63	–0.14	–0.39	–0.06	0.23
Ga	0.03	0.22	0.67	0.73	–0.15	–0.03	–0.25	–0.22	–0.23	–0.34	0.12	0.45	0.16	0.52	0.25	0.49	0.36	0.45	–0.44	–0.66	–0.08	0.25
Mo	–0.17	–0.09	0.14	0.28	0.72	0.42	–0.18	0.05	–0.45	–0.35	0.07	0.23	–0.13	0.06	–0.22	–0.15	0.24	0.39	0.14	–0.01	0.29	0.71
Ni	0.04	0.25	0.38	0.42	0.48	0.37	–0.30	–0.14	–0.56	–0.60	0.20	0.28	–0.08	0.22	–0.04	0.12	0.21	0.30	–0.17	–0.36	0.26	0.70
Ag	–0.07	–0.04	0.58	0.65	0.29	0.40	–0.13	0.07	–0.48	–0.49	0.48	0.67	0.12	0.51	0.01	0.14	0.38	0.64	–0.25	–0.44	0.04	0.37
V	–0.16	–0.04	0.37	0.62	0.01	0.07	–0.30	–0.27	–0.02	–0.26	–0.05	0.29	–0.01	0.34	0.04	0.33	0.26	0.40	–0.30	–0.60	–0.02	0.20
Zn	0.20	–0.26	–0.20	0.01	0.11	0.67	–0.23	–0.23	–0.16	–0.15	0.14	0.20	–0.04	0.05	0.54	–0.06	–0.27	–0.03	–0.17	–0.26	–0.20	–0.01

R – Pearson's linear coefficient, S – Spearman nonparametric.

and cobalt, copper, molybdenum, and silver can be described as negative linear correlations. Na_2O exhibits only non-parametric correlations, and statistically significant relationships occur for antimony, cobalt, copper, gallium, and silver, and are positive in nature. K_2O, similar to Na_2O, exhibits only non-parametric correlations, and these are few in number, as it is positively correlated with gallium and silver. TiO_2 is an oxide with two statistically significant positive correlations; it is linearly correlated with zinc and non-parametrically correlated with gallium. P_2O_5, similar to K_2O and Na_2O, exhibits non-parametric correlations, as this oxide is correlated with antimony, cobalt, copper, gallium, silver, and vanadium. MnO exhibits negative non-parametric correlations, as this oxide is correlated with cobalt, gallium, silver, and vanadium. Finally, Cr_2O_3 is only correlated with two elements – molybdenum and nickel – and these correlations are non-parametric in nature.

In summary, zinc did not exhibit correlations with other elements, but relationships with oxides (Fe_2O_3 and TiO_2) are observed. Antimony, similar to the element-element correlations, also exhibits non-parametric correlations with oxides. Vanadium is an element with few correlations, including those with oxides. The remaining correlations have a mixed nature, indicating complex relationships between the elements determined in coal ash and their oxide composition.

2.3. Regression models

The presence of numerous statistically significant correlations between coal ash and oxide variables implies a potential for developing regression models that can elucidate the relationships between these parameters (Table 4). To account for the complex interactions and dependencies in the dataset, multiple regression models with variable selection were implemented using the R package "leap", accompanied by hyperparameter tuning to optimize model performance. Additionally, a support vector machine (SVM) model was selected, also incorporating variable selection with "leap" and hyperparameter tuning, to capture both linear and non-linear relationships within the dataset. Due to the limited sample size and the large number of independent variables (oxides), it was deemed prudent to forego data splitting into training and testing sets, as this could lead to overfitting resulting from the constrained size of the training set, thereby compromising model generalizability.

Frequent appearance of Al_2O_3 and Fe_2O_3 as predictors across both linear and SVM models indicates their dominant role in governing trace metal behavior. Additionally, despite high MAPE (i.e., mean absolute percentage error) in the Zn model, strong R^2 (i.e., coefficient of determination) in SVM suggests effective learning of outlier-driven patterns, warranting the inclusion of hybrid modeling strategies (Tables 5, 6).

The R^2 values for most multiple regression models range from 0.17 (V) to 0.88 (Mo). The models for individual elements also differ in complexity, with the models for gallium and vanadium containing only one independent variable, while the models for molybdenum, nickel, and zinc have up to four independent variables. The models for gallium and vanadium,

which have only one independent variable, exhibit low explained variance (R^2), and the independent variable for these models was Al_2O_3. Models with three or four independent variables achieve the highest R^2 values.

Al_2O_3 is an independent variable in six models, including two where it is the sole independent variable. Fe_2O_3 appears as an independent variable in four models (see Table 5). Na_2O is an independent variable for antimony and zinc models, while K_2O is used in copper and nickel models, TiO_2 in nickel and zinc models, MnO in molybdenum and nickel models, and Cr_2O_3 in molybdenum and zinc models.

In addition to the large differences in model quality as measured by R^2, the models exhibit high variability in their performance on the test set. RMSE (i.e., root mean square error) values range from 0.36 for silver to 398 for vanadium. Similarly, MAPE shows a large spread of values. The performance on the test set is unacceptable (less than 10%) for all elements, and for four elements – antimony, cobalt, vanadium, and zinc – it exceeds 100%. This indicates poor model fit and the presence of numerous outliers in the test set. In the case of vanadium and zinc, high RMSE and MAPE values are associated with very high maximum values and standard deviations (Table 2).

Table 5. Multiple regression models for coal ash

Tabela 5. Modele regresji wielorakiej dla popiołów węgla

Y	Function	R^2	RMSE	MAPE %
Sb	$0.60 + 0.18 \times Fe_2O_3 + 1.41 \times Na_2O$	0.71	2.71	106.60
Co	$-21.24 + 4.64 \times Al_2O_3$	0.30	75.15	137.71
Cu	$-114.95 + 13.19 \times Al_2O_3 + 4.84 \times Fe_2O_3 - 75.01 \times K_2O$	0.80	66.49	58.55
Ga	$4.56 + 1.76 \times Al_2O_3$	0.51	18.65	40.73
Mo	$-9.79 + 1.19 \times Fe_2O_3 + 4.73 \times P_2O_5 - 50.44 \times MnO + 163.33 \times Cr_2O_3$	0.88	6.58	63.36
Ni	$550.58 - 13.97 \times CaO - 97.45 \times K_2O - 126.04 \times TiO_2 - 368.04 \times MnO$	0.75	67.13	34.37
Ag	$-0.41 + 0.03 \times Al_2O_3 + 0.02 \times Fe_2O_3$	0.54	0.36	81.11
V	$122.32 + 16.89 \times Al_2O_3$	0.17	398.30	115.49
Zn	$313.10 - 30.59 \times Al_2O_3 + 103.12 \times Na_2O + 633.37 \times TiO_2 - 3747.40 \times Cr_2O_3$	0.79	210.30	1,665.35

In all statistically significant support vector machine (SVM) models, the parameters nu = 0.5 and epsilon = 0.1 were employed. The remaining parameters and model performance are presented in Table 6 for ash.

SVM models generally exhibited higher coefficients of determination (R^2) compared to multiple regression models. The most significant difference in model quality is observed for the elements: silver (Ag) and vanadium (V), with differences of 0.28 and 0.32, respectively

(Tables 5, 6). The calculated mean absolute percentage error (MAPE) values also indicate better performance of the SVM models. For copper (Cu), molybdenum (Mo), nickel (Ni), vanadium (V), and zinc (Zn), the MAPE values for the SVM models are substantially lower than those for the multiple regression models.

An analysis of the independent variables reveals frequent occurrences of Al_2O_3 and Fe_2O_3 as components of the model. The multiple regression and SVM models share a common set of independent variables for the elements antimony (Sb), cobalt (Co), copper (Cu), gallium (Ga), nickel (Ni), silver (Ag), and zinc (Zn). In the case of molybdenum, Fe_2O_3, P_2O_5, and MnO are common to both models, while the multiple regression model includes additional Cr_2O_3, and the SVM model includes TiO_2 and K_2O. The multiple regression model for vanadium includes only Al_2O_3, whereas the SVM model includes additional Fe_2O_3 and Na_2O (Tables 5, 6).

Table 6. Support vector machine (SVM) models for coal ash

Tabela 6. Modele maszyny wektorów nośnych (SVM) dla popiołów węgla

Y	X	R^2	Model parameters	MAPE
Sb	Fe_2O_3, Na_2O	0.74	gamma = 0.5, rho = –0.51	98.13
Co	Al_2O_3	0.32	gamma = 1.0, rho = 0.18	98.11
Cu	Al_2O_3, Fe_2O_3, K_2O	0.94	gamma = 0.33, rho = –0.14	21.31
Ga	Al_2O_3	0.56	gamma = 1.0, rho = –0.11	28.30
Mo	Fe_2O_3, P_2O_5, TiO_2, MnO, K_2O	0.86	gamma = 0.2, rho = –0.05	36.94
Ni	CaO, K_2O, TiO_2, MnO	0.87	gamma = 0.25, rho = 0.28	19.78
Ag	Al_2O_3, Fe_2O_3	0.82	gamma = 0.5, rho = –0.01	32.17
V	Al_2O_3, Fe_2O_3, Na_2O	0.49	gamma = 0.33, rho = –0.24	45.86
Zn	Al_2O_3, Na_2O, TiO_2, Cr_2O_3	0.92	gamma = 0.25, rho = –0.05	50.12

3. Discussion

In this study, the content of nine key elements (Cu, Co, Ni, V, Sb, Mo, Zn, Ag, Ga) was analyzed in 28 coal samples and their ashes. The results indicate a significant redistribution of elements during combustion, with concentrations of certain metals in coal ash being higher than in the original coal (Appendix 1). Interestingly, bituminous coals exhibited higher concentrations of copper, cobalt, and silver, while lignites had increased levels of zinc and nickel. The combustion process led to the enrichment of metals such as nickel, vanadium,

and copper in the ash. The highest total metal content in ash was observed in sample 15B (bituminous, 2576.3 ppm total metal content), while the highest zinc concentration was found in sample 14L (lignite, 1818 ppm Zn). The redistribution of elements in ash suggests that some metals volatilize and condense on ash particles, resulting in selective enrichment. This is consistent with the different volatility of elements (Bielowicz et al. 2018). The observed enrichment of nickel, vanadium, copper, and zinc is primarily controlled by their moderate volatility and strong affinity for aluminosilicate and iron-bearing mineral phases. During combustion, metals originally bound to organic matter or sulfides are released into the gas phase and subsequently recondense on fine ash particles, especially on fly ash fractions, leading to secondary enrichment.

A review of the literature reveals that combustion significantly alters the distribution of metals in coal. Asokan et al. (2005) found that fly ash is typically enriched in elements such as arsenic, boron, and lead, with enrichment factors exceeding those in parent coal. This is consistent with our study, where ash samples exhibited much higher concentrations of non-volatile metals, such as vanadium (1426.0 ppm in sample 4L) and nickel (466.2 ppm in sample 10B), compared to their coal counterparts, which contained 69.0 ppm vanadium and 59.0 ppm nickel, respectively. The enrichment factors observed for nickel in coal ash were almost ten times higher than in the original coal, consistent with the results of Wang (2019). They noted a similar increase in metal content after combustion. Further comparison with global Clarke values reported by Ketris and Yudovich (2009) for coal provides additional insights into the distribution of trace elements. The average copper (Cu) concentration in coal samples was 14.5 ppm, significantly lower than the Clarke value of 60 ppm, indicating depletion of this element compared to global averages, while in ash the average concentration increased to 176.9 ppm, reaching 60.6 ppm in lignite and up to 250.4 ppm in bituminous ash. Similarly, cobalt (Co) concentrations averaged 4.5 ppm, much lower than the Clarke value of 25 ppm, suggesting significant depletion of these coal samples. However, in ash, a clear enrichment was observed, with the average concentration increasing to 71.0 ppm, including 28.3 ppm in lignite and 108.3 ppm in bituminous ash. Additionally, zinc (Zn) concentrations in lignite coal samples reached 454.2 ppm (sample 14L), significantly exceeding the Clarke value of 70 ppm, indicating large variability in Zn distribution among different coal types. The highest zinc concentration in ash was likewise recorded for sample 14L, reaching 1818 ppm, which indicates strong enrichment during combustion. However, antimony (Sb) exhibits low average concentrations in coal, not exceeding 0.37 ppm, compared to the Clarke value of 1.2 ppm. In contrast, ash is enriched, with an average concentration of 4.1 ppm; however, it is worth noting that in lignite samples, the average content remains lower, at 0.63 ppm. These discrepancies between Clarke values and measured concentrations clearly demonstrate that ash geochemistry is strongly site-specific and controlled by both geological provenance and combustion technology. Therefore, universal average values cannot be directly applied to environmental risk assessment or resource evaluation without local verification. The clear geochemical contrast between lignite- and bituminous-derived ashes further supports the role of coal rank as a first-order control on trace metal behavior.

Bituminous coal ashes are enriched in copper, cobalt, and silver, likely due to stronger association of these elements with sulfide phases and organic matter, whereas higher zinc content in lignite ashes reflects a stronger influence of detrital and carbonate mineral fractions.

Additional insights derived from the results include the need for local geochemical assessments prior to the reuse of coal ashes due to the considerable variability in trace metal content. The improved predictive performance of non-linear modeling approaches (e.g., SVM) suggests that non-linear dependencies between metals and oxides are prevalent and should be considered in environmental and industrial forecasting tools. Given the strong associations between specific oxides (Al_2O_3, Fe_2O_3, Cr_2O_3) and trace elements, these oxides may serve as proxy indicators for preliminary assessments of ash resource potential. Samples identified as statistical outliers may represent valuable sources of strategic metals and merit further targeted investigation. The elevated concentrations of critical raw materials such as vanadium (V), gallium (Ga), cobalt (Co), and molybdenum (Mo) clearly indicate that selected coal ashes may constitute a realistic secondary resource base, provided that appropriate recovery technologies are applied.

The correlation analysis provided additional insights into the geochemical behavior of the discussed metals. Strong correlations were observed between cobalt and silver ($R = 0.96$) and between copper and cobalt ($R = 0.90$), suggesting common geochemical affinities. These relationships indicate that some trace elements tend to co-occur in coal and persist during combustion. Dai and Finkelman (2018) reported that elements like gallium (Ga) and vanadium (V) exhibit distinct geochemical behaviors depending on coal rank and combustion conditions, consistent with our findings. The statistical analysis also identified Al_2O_3, Fe_2O_3, and Cr_2O_3 as key predictors of metal distribution in coal and ash, confirming the hypothesis that metal accumulation is largely dependent on mineralogical composition. Multiple regression models further reinforced these findings, with high predictive accuracy for several metals. SVM modeling demonstrated particularly strong predictive capability for copper (Cu), zinc (Zn), and nickel (Ni), with R^2 values of 0.94, 0.92, and 0.87, respectively.

While several models exhibited high MAPE values, in some cases exceeding 100%, this should not be interpreted solely as evidence of poor model structure. In datasets characterized by strong heterogeneity, skewed distributions, and the presence of extreme values – as is typical for trace element concentrations in coal ash – MAPE becomes highly sensitive to low denominators and anomalously high observations. Consequently, even models with high coefficients of determination (R^2) may yield inflated MAPE values when rare but extreme concentrations occur. In this context, R^2 provides a more robust measure of model goodness-of-fit, as it reflects the proportion of variance explained by the model across the entire dataset. The consistently high R^2 values obtained for several elements, particularly in the SVM models (e.g., Cu: $R^2 = 0.94$; Zn: $R^2 = 0.92$; Ni: $R^2 = 0.87$; Mo: $R^2 = 0.86$), indicate that the underlying relationships between oxides and trace metals were effectively captured, despite the presence of outliers.

High MAPE values observed for selected elements (notably Zn, Co, V, Sb) in multiple regression models are therefore interpreted as indicators of strong local anomalies rather

than systematic model failure. Such anomalies are geochemically meaningful, as they may reflect episodic enrichment events, mineralogical heterogeneity, or localized concentration of strategic metals. From the perspective of resource assessment, these outlier-driven patterns are particularly important, as they may signal materials with elevated recovery potential rather than noise that should be suppressed.

The comparison between multiple regression and SVM approaches demonstrates that non-linear models are better suited to handling such complexity. SVM models consistently reduced MAPE while maintaining or improving R^2 values relative to linear regression, confirming that non-linear dependencies dominate oxide–metal interactions in coal ash systems. These findings highlight the necessity of combining classical statistical metrics with a critical understanding of data structure when evaluating model performance in environmental geochemistry. These results indicate that it is possible to predict metal concentrations in coal ash based on elemental composition. The models developed in this study highlight the complex interactions between trace elements during combustion and suggest that predictive modeling can be a valuable tool for assessing the distribution of metals in different coal types. From a practical perspective, the superior performance of SVM models demonstrates that machine-learning techniques are better suited for ash geochemical forecasting than classical linear regression, especially in datasets characterized by strong heterogeneity and outliers.

Conclusions

The analytical results obtained in this study demonstrate that the combustion of coal leads to a substantial redistribution and enrichment of trace elements in the resulting ash, with non-volatile metals, including vanadium (V), nickel (Ni), and zinc (Zn), exhibiting pronounced accumulation. A comparative analysis of Clarke's values for coal and ash, as well as Earth's crust Clarke values, reveals the depletion of certain elements in coal and their subsequent enrichment in ash, thereby illustrating the influence of combustion on elemental concentration. The observed discrepancies underscore the importance of conducting local assessments of coal composition and combustion residues to enhance predictions of environmental impact and potential recovery of critical elements. Furthermore, correlation and regression analyses highlight the geochemical relationships between elements and suggest that the modeling approaches employed can provide valuable insights into the distribution of trace metals in coal and ash. Ultimately, these findings underscore the need for developing technologies aimed at recovering valuable metals, such as vanadium (V) and gallium (Ga), which exhibit significant accumulation in ash residues. The strong statistical importance of Al_2O_3 and Fe_2O_3 as predictors confirms that aluminosilicate and iron-bearing phases dominate trace metal retention mechanisms in coal ash and control the long-term mobility and environmental behavior of metals. The very high variability of trace metal concentrations, including extreme outliers, indicates that coal ashes cannot be treated as

geochemically uniform materials, which has direct implications for environmental safety regulations, waste classification procedures, and decisions regarding industrial reuse. At the same time, the enrichment of strategic metals such as vanadium (V), gallium (Ga), cobalt (Co), and molybdenum (Mo) confirms that selected ashes represent a promising secondary resource that may support circular economy strategies and raw material security, especially in the context of limited primary deposits within the European Union. The superior performance of support vector machine (SVM) models compared to multiple regression demonstrates that non-linear relationships dominate the oxide–metal system in coal ash and that machine-learning-based approaches provide a more reliable tool for forecasting trace metal distributions in highly heterogeneous datasets. The consistently high R^2 values obtained for several trace elements, especially in SVM models, confirm that the dominant geochemical controls governing metal distribution were successfully identified. Elevated MAPE values observed alongside high R^2 are interpreted as evidence of pronounced anomalous observations rather than inadequate model structure. Importantly, these anomalies are not merely statistical artifacts but may represent ash fractions with enhanced concentrations of critical or strategic metals, which are of particular interest from a circular economy and resource recovery perspective.

The applied statistical framework can therefore be used as an effective screening tool for large ash repositories, enabling the rapid identification of materials with the greatest technological potential for critical metal recovery. In a broader perspective, the integration of geochemical characterization, statistical modeling, and circular economy concepts offers a comprehensive strategy for transforming coal combustion residues from environmental burdens into valuable secondary raw material resources. Future research should focus on extending the dataset to include different combustion technologies and geographic regions, as well as on the verification of recovery efficiencies using hydrometallurgical and bioleaching methods under industrial-scale conditions.

Future research should focus on expanding the dataset to include ashes derived from different combustion technologies (fluidized bed, gasification) and a broader range of geological settings. Further studies should also verify statistically predicted metal recoverability using laboratory-scale hydrometallurgical and bioleaching experiments, as well as assess long-term leaching behavior under environmental conditions. This will allow the direct linking of predictive models with technological feasibility and environmental risk assessment.

Appendix 1. Raw data (ppm)

Załącznik 1. Dane surowe (ppm)

ID	Sb		Co		Cu		Ga		Mo		Ni		Ag		V		Zn	
	coal	ash	coal	ash	coal	ash	coal	ash	coal	ash	coal	ash	coal	ash	coal	ash	coal	ash
1L	0.21	0.2	3.7	9.6	16.3	34.2	2.6	17.5	7.9	17.3	185.7	113.3	0.03	0.10	12.0	70.0	11.6	22.0
2L	0.06	I.S.	1.0	19.1	2.7	I.S.	0.6	15.8	0.6	I.S.	14.5	I.S.	0.01	I.S.	11.0	231.0	45.7	I.S.
3L	0.09	0.6	2.5	10.5	10.5	36.2	0.7	4.5	3.6	16.5	89.9	190.6	0.02	0.10	6.0	27.0	10.5	29.0
4L	0.44	I.S.	5.7	104.7	3.4	I.S.	1.3	34.8	0.6	I.S.	14.3	I.S.	0.01	I.S.	69.0	1,426.0	17.2	I.S.
5L	0.11	I.S.	2.7	76.5	4.8	I.S.	0.9	30.1	0.3	I.S.	11.7	I.S.	0.00	I.S.	20.0	559.0	20.6	I.S.
7L	0.02	I.S.	0.4	7.7	1.7	I.S.	0.4	5.4	0.2	I.S.	5.3	I.S.	0.00	I.S.	3.0	69.0	4.5	I.S.
9L	0.03	0.4	0.3	4.3	1.4	96.9	0.3	3.9	0.2	3.8	1.6	26.5	0.01	0.10	2.0	31.0	58.9	559.0
10L	0.06	0.5	2.3	15.4	5.9	63.2	3.6	31.9	0.5	4.0	7.9	66.4	0.02	0.10	18.0	162.0	17.9	138.0
11L	0.09	1.2	1.1	16.9	3.9	47.5	6.2	93.7	0.4	7.2	7.9	77.5	0.01	0.20	90.0	1,404.0	16.5	126.0
12L	0.18	0.8	4.5	23.5	11.9	72.8	5.4	32.2	1.2	6.9	15.9	75.5	0.03	0.20	58.0	363.0	30.4	116.0
13L	0.04	I.S.	0.5	20.6	2.8	I.S.	0.6	23.8	0.4	I.S.	4.9	I.S.	0.01	I.S.	4.0	178.0	11.5	I.S.
14L	0.20	0.7	7.4	30.7	15.2	73.4	5.0	33.3	0.5	2.8	25.4	89.9	0.05	0.20	25.0	176.0	454.2	1,818.0
1SB	0.09	0.3	5.5	24.4	8.8	35.4	3.1	19.6	0.6	3.3	20.5	67.8	0.02	0.10	37.0	226.0	22.0	68.0
1B	1.67	10.1	3.1	114.4	25.0	422.0	0.8	82.3	1.0	17.3	6.2	301.6	0.05	0.90	11.0	626.0	12.1	236.0
3B	0.68	14.7	7.3	107.5	22.7	289.2	3.9	54.8	1.3	32.0	27.7	243.3	0.10	1.20	17.0	277.0	41.8	202.0
4B	1.06	14.9	3.7	63.2	8.2	162.6	1.7	39.4	0.6	17.3	26.4	260.2	0.07	1.00	12.0	227.0	121.6	914.0
5B	0.44	5.0	7.3	97.1	18.2	236.9	2.6	51.7	0.9	19.7	21.6	194.9	0.09	1.20	37.0	554.0	34.4	258.0
6B	0.71	1.4	4.3	19.1	29.3	106.8	4.0	44.4	1.1	3.6	16.6	80.2	0.09	0.30	44.0	285.0	12.4	66.0
9B	0.34	8.3	3.2	33.7	14.6	201.5	0.6	11.5	2.1	38.5	19.9	169.5	0.03	0.30	15.0	210.0	9.0	96.0
10B	1.30	9.5	11.4	93.9	31.4	335.6	1.8	33.1	5.9	68.7	59.0	466.2	0.14	1.10	45.0	539.0	15.9	164.0
11B	0.53	I.S.	9.6	360.0	18.7	I.S.	0.8	55.0	2.2	I.S.	23.2	I.S.	0.03	I.S.	26.0	1,112.0	16.5	I.S.
12B	0.72	I.S.	9.5	326.4	34.6	I.S.	0.7	47.4	2.4	I.S.	25.5	I.S.	0.05	I.S.	35.0	1,277.0	9.4	I.S.
15B	0.23	4.5	9.2	180.6	23.3	461.0	3.1	110.4	2.0	47.2	26.8	406.7	0.13	1.90	56.0	1,234.0	6.0	130.0
16B	0.19	1.8	8.0	92.7	38.2	437.5	3.2	74.9	1.7	23.1	25.3	257.1	0.11	1.00	39.0	545.0	6.2	110.0
17B	0.25	6.5	3.4	30.8	12.3	146.7	3.4	31.7	0.6	11.5	13.3	86.6	0.06	0.50	17.0	193.0	5.3	50.0
18B	0.19	1.3	1.9	15.8	14.7	148.8	2.9	42.3	0.5	6.4	7.2	54.6	0.05	0.30	23.0	261.0	7.8	67.0
19B	0.20	1.6	2.5	29.7	13.0	156.4	1.2	43.4	0.7	8.0	6.4	99.2	0.04	0.40	19.0	287.0	6.0	82.0
20B	0.14	1.6	3.2	58.6	12.6	149.9	0.8	40.6	0.5	6.6	5.8	106.1	0.03	0.40	15.0	280.0	10.5	97.0
Clarke Earth Crust	1.20	1.2	25.0	25.0	60.0	60.0	12.0	12.0	1.5	1.5	84.0	84.0	0.00	0.12	120.0	120.0	70.0	70.0

This research project was partly supported by the AGH University of Krakow, Faculty of Geology, Geophysics and Environmental Protection, as a part of a statutory project.

The Authors have no conflict of interest to declare.

REFERENCES

Akinyemi et al. 2020 – Akinyemi, S.A., Adebayo, O.F., Nyakuma, B.B., Adegoke, A.K., Aturamu, O.A., OlaOlorun, O.A., Adetunji, A., Hower, J.C., Hood, M.M. and Jauro, A. 2020. Petrology, physicochemical and thermal analyses of selected cretaceous coals from the Benue Trough Basin in Nigeria. *International Journal of Coal Science & Technology* 7(1), pp. 26–42, https://doi.org/10.1007/s40789-020-00303-6.

Asokan et al. 2005 – Asokan, P., Saxena, M. and Asolekar, S.R. 2005. Coal combustion residues – environmental implications and recycling potentials. *Resources, Conservation and Recycling* 43(3), pp. 239–262, https://doi.org/10.1016/j.resconrec.2004.06.003.

Bielowicz et al. 2018 – Bielowicz, B., Botor, D., Misiak, J. and Wagner, M. 2018. Critical Elements in Fly Ash from the Combustion of Bituminous Coal in Major Polish Power Plants. *E3S Web of Conferences*, https://doi.org/10.1051/e3sconf/20183502003.

Dagwar et al. 2025 – Dagwar, P.P., Iqbal, S.S. and Dutta, D. 2025. Sustainable recovery of rare Earth elements from industrial waste: A path to circular economy and environmental health. *Waste Management Bulletin* 3(1), pp. 373–390, https://doi.org/10.1016/j.wmb.2025.02.004.

Dai, S. and Finkelman, R.B. 2018. Coal as a promising source of critical elements: Progress and future prospects. *International Journal of Coal Geology* 186, pp. 155–164, https://doi.org/10.1016/j.coal.2017.06.005.

Dai et al. 2012 – Dai, S., Ren, D., Chou, C.L., Finkelman, R.B., Seredin, V.V. and Zhou, Y. 2012. Geochemistry of trace elements in Chinese coals: A review of abundances, genetic types, impacts on human health, and industrial utilization. *International Journal of Coal Geology* 94, pp. 3–21, https://doi.org/10.1016/j.coal.2011.02.003.

Font et al. 2007 – Font, O., Querol, X., Juan, R., Casado, R., Ruiz, C.R., López-Soler, Á., Coca, P. and Peña, F.G. 2007. Recovery of gallium and vanadium from gasification fly ash. *Journal of Hazardous Materials* 139(3), pp. 413–423, https://doi.org/10.1016/j.jhazmat.2006.02.041.

Franus et al. 2015 – Franus, W., Wiatros-Motyka, M.M. and Wdowin, M. 2015. Coal fly ash as a resource for rare earth elements. *Environmental Science and Pollution Research* 22(12), pp. 9464–9474, https://doi.org/10.1007/s11356-015-4111-9.

Gaustad et al. 2021 – Gaustad, G., Williams, E. and Leader, A. 2021. Rare earth metals from secondary sources: Review of potential supply from waste and byproducts. *Resources, Conservation and Recycling* 167, https://doi.org/10.1016/j.resconrec.2020.105213.

Harkness et al. 2015 – Harkness, J.S., Ruhl, L.S., Millot, R., Kloppman, W., Hower, J.C., Hsu-Kim, H. and Vengosh, A. 2015. Lithium Isotope Fingerprints in Coal and Coal Combustion Residuals from the United States. *Procedia Earth and Planetary Science* 13, pp. 134–137, https://doi.org/10.1016/j.proeps.2015.07.032.

Hauke, J. and Kossowski, T. 2011. Comparison of Values of Pearson's and Spearman's Correlation Coefficients on the Same Sets of Data. *Quaestiones Geographicae* 30(2), pp. 87–93, https://doi.org/10.2478/v10117-011-0021-1.

Izquierdo et al. 2013 – Izquierdo, M., Tye, A.M. and Chenery, S.R. 2013. Measuring reactive pools of Cd, Pb and Zn in coal fly ash from the UK using isotopic dilution assays. *Applied Geochemistry* 33, pp. 41–49, https://doi.org/10.1016/j.apgeochem.2013.01.013.

Joshi et al. 2025 – Joshi, K., Magdouli, S. and Brar, S.K. 2025. Bioleaching for the recovery of rare earth elements from industrial waste: A sustainable approach. *Resources, Conservation and Recycling* 215, https://doi.org/10.1016/j.resconrec.2025.108129.

Ketris, M.P. and Yudovich, Ya.E. 2009. Estimations of Clarkes for Carbonaceous biolithes: World averages for trace element contents in black shales and coals. *International Journal of Coal Geology* 78(2), pp. 135–148, https://doi.org/10.1016/j.coal.2009.01.002.

Lefticariu et al. 2020 – Lefticariu, L., Klitzing, K.L. and Kolker, A. 2020. Rare Earth Elements and Yttrium (REY) in coal mine drainage from the Illinois Basin, USA. *International Journal of Coal Geology* 217, https://doi.org/10.1016/j.coal.2019.103327.

Marshall, G. and Jonker, L. 2010. An introduction to descriptive statistics: A review and practical guide. *Radiography* 16(4), pp. 1–7, https://doi.org/10.1016/j.radi.2010.01.001.

Pan et al. 2018 – Pan, J., Zhou, C., Liu, C., Tang, M., Cao, S., Hu, T., Ji, W., Luo, Y., Wen, M. and Zhang, N. 2018. Modes of Occurrence of Rare Earth Elements in Coal Fly Ash: A Case Study. *Energy & Fuels* 32(9), pp. 9738–9743, https://doi.org/10.1021/acs.energyfuels.8b02052.

Quina et al. 2018 – Quina, M.J., Bontempi, E., Bogush, A., Schlumberger, S., Weibel, G., Braga, R., Funari, V., Hyks, J., Rasmussen, E. and Lederer, J. 2018. Technologies for the management of MSW incineration ashes from gas cleaning: New perspectives on recovery of secondary raw materials and circular economy. *Science of The Total Environment* 635, pp. 526–542, https://doi.org/10.1016/j.scitotenv.2018.04.150.

Seredin, V.V. 1996. Rare earth element-bearing coals from the Russian Far East deposits. *International Journal of Coal Geology* 30(1–2), pp. 101–129, https://doi.org/10.1016/0166-5162(95)00039-9.

Wang et al. 2019 – Wang, T., Li, Y., Jin, L., Wang, D. and Hu, H. 2019. Steam catalytic cracking of coal tar over iron-containing mixed metal oxides. *Canadian Journal of Chemical Engineering* 97(3), pp. 702–708, https://doi.org/10.1002/cjce.23210.

Zhang et al. 2018 – Zhang, L., Tao, Y. and Yang, L. 2018. Research on flow field and kinematic characteristics of fly ash particles in rotary triboelectrostatic separator. *Powder Technology* 336, pp. 168–179, https://doi.org/10.1016/j.powtec.2018.05.055.

DESCRIPTIVE AND PREDICTIVE ANALYSIS OF TRACE METALS IN COAL ASH: STATISTICAL INSIGHTS AND MODELING

Keywords

coal, ash, regression models, exploratory data analysis, critical raw material

Abstract

Coal combustion generates ash that contains trace metals with both economic and environmental relevance. This study aims to assess the concentration, variability, and inter-element relationships of nine trace metals (Sb, Co, Cu, Ga, Mo, Ni, Ag, V, Zn) in ash samples from 28 coal specimens of varying rank (lignite, subbituminous, and bituminous) collected from Polish deposits. Elemental concentrations were determined via ICP-MS, and oxide composition was analyzed to examine geochemical associations. Descriptive statistics, correlation analysis, and predictive modeling (multiple linear regression and Support Vector Machine, SVM) were applied to characterize elemental behavior and identify reliable predictors of metal content in ash. The results show substantial variability in elemental concentrations, with several metals (e.g., Ni, V, Zn) enriched in ash relative to parent coal. Bituminous coal ashes generally exhibited higher average concentrations than lignite ashes, except for Zn. Strong linear correlations were found between selected metal pairs (e.g., Cu–Co, Ag–Co), while correlations with oxides (notably Al_2O_3, Fe_2O_3, Cr_2O_3) supported their role in controlling metal distribution. Regression models demonstrated predictive capability for most elements (R2 up to 0.88), with SVM models showing improved performance (R^2 up to 0.94, MAPE as low as 19.78%). These findings highlight the importance of oxide composition in trace metal behavior and provide a methodological basis for assessing ash quality, environmental risk, and potential resource recovery.

ANALIZA OPISOWA I PREDYKCYJNA METALI ŚLADOWYCH W POPIOŁACH ZE SPALANIA WĘGLA: UJĘCIE STATYSTYCZNE I MODELOWANIE

Słowa kluczowe

węgiel, popiół, modele regresyjne, eksploracyjna analiza danych, pierwiastki krytyczne

Streszczenie

Spalanie węgla generuje popioły zawierające pierwiastki śladowe o istotnym znaczeniu gospodarczym i środowiskowym. Celem niniejszego badania była ocena stężenia, zmienności oraz relacji pomiędzy dziewięcioma metalami śladowymi (Sb, Co, Cu, Ga, Mo, Ni, Ag, V, Zn) w próbkach popiołów uzyskanych z 28 próbek węgla o różnym stopniu uwęglenia (węgiel brunatny, brunatny twardy i kamienny) pochodzących z polskich złóż. Stężenia pierwiastków oznaczono metodą ICP-MS, a analizę składu tlenkowego przeprowadzono w celu identyfikacji powiązań geochemicznych. Wykorzystano statystyki opisowe, analizę korelacji oraz modele predykcyjne (regresja liniowa wieloraka i maszyny wektorów nośnych – SVM) do scharakteryzowania zachowania pierwiastków i wskazania niezawodnych predyktorów ich zawartości w popiele. Wyniki wykazały znaczną zmienność stężeń pierwiastków, przy czym niektóre metale (np. Ni, V, Zn) uległy wzbogaceniu w popiele względem węgla macierzystego. Popioły z węgla kamiennego zawierały przeciętnie wyższe stężenia metali niż z węgla brunatnego, z wyjątkiem cynku. Zaobserwowano silne korelacje liniowe pomiędzy wybranymi parami metali (np. Cu–Co, Ag–Co) oraz istotne związki z tlenkami (zwłaszcza Al_2O_3, Fe_2O_3, Cr_2O_3), co potwierdza ich wpływ na rozkład metali. Modele regresji wykazały dobrą zdolność predykcyjną (R2 do 0,88), a modele SVM uzyskały jeszcze lepsze wyniki (R^2 do 0,94, MAPE nawet 19,78%). Uzyskane wyniki podkreślają znaczenie składu tlenkowego w analizie zachowania pierwiastków śladowych i dostarczają metodycznych podstaw do oceny jakości popiołu, ryzyka środowiskowego i możliwości odzysku surowców.